Polymer 50 (2009) 177–188

Contents lists available at ScienceDirect

Polymer

journal homepage: www.elsevier.com/locate/polymer

DNA-like interactions enhance the miscibility of supramolecular polymer blends

Shiao-Wei Kuo*, Ren-Shin Cheng

Department of Materials and Optoelectronic Engineering, Center for Nanoscience and Nanotechnology, National Sun Yat-Sen University, Kaohsiung 804, Taiwan

ARTICLE INFO

Article history:
Received 16 September 2008
Received in revised form
26 October 2008
Accepted 27 October 2008
Available online 5 November 2008

Keywords:
Hydrogen bonding
Miscibility
Supramolecule

ABSTRACT

We have investigated the miscibility behavior, specific interactions, and supramolecular structures of blends of the DNA-like copolymers poly(vinylbenzylthymine-*co*-butyl methacrylate) (T-PBMA) and poly(vinylbenzyladenine-*co*-styrene) (A-PS) with respect to their vinylbenzylthymine (VBT) and vinylbenzyladenine (VBA) contents. ^{1}H nuclear magnetic resonance spectroscopy and one- and two-dimensional Fourier transform infrared spectroscopy revealed that hydrogen bonding occurred exclusively between the VBA and VBT units. In addition, size exclusion chromatography, dynamic light scattering, and viscosity analyses provided evidence for the formation of supramolecular network structures in these binary blend systems. A miscibility window existed in the A-PS/T-PBMA blend system when the VBT and VBA fractions in the copolymers were greater than 11 mol%, as predicted using the Painter–Coleman association model.

1. Introduction

One approach toward preparing new materials exhibiting tunable properties is the blending of two or more polymers [1]. Indeed, polymer blending is a powerful route toward materials exhibiting properties and cost performances superior to those of their individual components. Unfortunately, most polymer blends are immiscible because of their high degrees of polymerization; as a result, the entropic term becomes vanishingly small and the miscibility becomes increasingly dependent on the contribution of the enthalpic term. To enhance the formation of miscible one-phase systems of polymer blends, it is necessary for favorable specific intermolecular interactions to exist between the two (or more) base components of the blend. Many attempts have been made to decrease the interfacial energy and reduce the propensity for polymer blends to undergo phase separation, including the use of compatibilizers such as block and graft copolymers [2,3]. Another approach involves introducing functional groups to connect individual polymer main chains together noncovalently using, for example, hydrogen bonding, dipole–dipole, and π–π interactions [4–11]. The miscibility of an immiscible blend can be enhanced by introducing a functional group to one component to enable the formation of intermolecular interactions with another [12].

In previous studies of the roles of intermolecular association in miscibility enhancement, we found that the incorporation of a large number of hydrogen bond acceptors (ca. 45 mol% of polyacetoxystyrene) or donors (ca. 13 mol% of polyvinylphenol) into a polystyrene (PS) chain renders the modified polymer miscible with phenolic resin (a well-known hydrogen bonding donor) [13] or poly(ε-caprolactone) (a well-known hydrogen bonding acceptor) [14], respectively. If the monomers possess relatively weak hydrogen bonding moieties (e.g., hydroxyl, carboxyl, pyridyl, or ether groups), then the corresponding weak intermolecular interactions require a relatively high mole percentage of the copolymer to induce miscibility, resulting in properties of the polymer blend that differ substantially from those of the unmodified polymer [15–19]. Ideally, adding low mole percentages of the recognition units into the two immiscible phases would result in a miscible phase.

Multiple hydrogen bonding arrays play a fundamental role in complex biological systems (e.g., DNA complexation). DNA is a very influential structure in polymer science, where it is often presented as a defined macromolecule possessing a nearly perfect molecular structure. As a result, the preparation of synthetic polymers that mimic DNA remains a very important challenge in polymer science [20]. The self-assembly of pairs of DNA strands is mediated by intermolecular hydrogen bonding between complementary purine [adenine (A) and guanine (G)] and pyrimidine [thymine (T) and cytosine (C)] bases attached to a phosphate sugar backbone: G binds selectively to C and A binds selectively to T [21]. Taking this cue from nature, we wondered whether we could enhance the miscibility of immiscible binary blends by preparing synthetic polymers possessing nucleotide bases on their side chains.

Our first challenge was developing methods for synthesizing DNA base-containing random copolymers using conventional free radical polymerization. As monomers, we chose 9-(4-

* Corresponding author. Tel.: +886 7 5252000x4079; fax: +886 7 5254099.
E-mail address: kuosw@faculty.nsysu.edu.tw (S.-W. Kuo).

0032-3861/$ – see front matter © 2008 Elsevier Ltd. All rights reserved.
doi:10.1016/j.polymer.2008.10.047

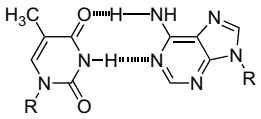

Scheme 1. Formation of strong multiple hydrogen bonding interactions between A and T units.

vinylbenzyl)adenine (VBA) and 1-(4-vinylbenzyl)thymine (VBT) because A and T have small self-association equilibrium constants (K_B = ca. 3 M^{-1}) [22] but form very strong complexes together (K_A = ca. 530 M^{-1}; Scheme 1) [23–25]. The aims of this study were (1) to investigate the miscibility of blends of the copolymers poly(vinylbenzylthymine-*co*-butyl methacrylate) (T-PBMA) and poly(vinylbenzyladenine-*co*-styrene) (A-PS), (2) to use spectroscopic methods to provide evidence for specific intermolecular association of the A and T units, and (3) to use the Painter–Coleman association model (PCAM) to predict whether a miscibility window exists for blends of T-PBMA and A-PS [26,27].

2. Experimental section

2.1. Materials

Styrene and *n*-butyl methacrylate (Aldrich, USA) were passed through an alumina column and then vacuum distilled from calcium hydride under reduced pressure prior to use. Vinylbenzyl chloride was purchased from Acros Organics (Germany) and distilled prior to use. Thymine and adenine were obtained from Aldrich (USA). DMF and DMSO were distilled from calcium hydride under vacuum prior to use. All other chemicals were of reagent grade and used as received without further purification.

2.1.1. 1-(4-Vinylbenzyl)thymine (VBT) [28,29]

Thymine (1.2 g) was dissolved at ambient temperature into a solution of potassium hydroxide (0.632 g) in distilled water (60 mL). The solvent was evaporated under reduced pressure while maintaining the temperature below 35 °C. Any residual water was removed through co-evaporation with dry DMF (20 mL). The resulting semi-solid residue was suspended in dry DMF (240 mL) under nitrogen at room temperature and then 4-vinylbenzyl chloride (1.46 g) and the inhibitor 2,6-di-*tert*-butyl-4-methylphenol (6 mg) were added. The well-stirred slurry was heated to 70 °C for 10 h and then cooled to room temperature. DMF was evaporated off under reduced pressure at temperatures below 35 °C. The residue was dissolved in boiling toluene (60 mL); the product that crystallized after cooling was collected through filtration (yield: ca. 50%; m.p. 180 °C).

2.1.2. 9-(4-Vinylbenzyl)adenine (VBA) [30]

4-Vinylbenzyl chloride (0.71 mL) was added to a stirred suspension of adenine (0.675 g), anhydrous potassium carbonate (0.76 g), potassium iodide (9 mg), and hydroquinone (10 mg) in DMF (10 mL) under an inert nitrogen atmosphere. The mixture was heated under reflux for 16 h and then hot-filtered; the collected solids were washed with hot DMF (10 mL). The combined filtrates were evaporated to dryness under vacuum. The residue was mixed with chloroform and filtered through silica gel. After evaporating the solvent, the product was recrystallized from methanol with addition of charcoal (yield: ca. 35%; m.p. 220 °C).

2.1.3. Poly(vinylbenzylthymine-co-butyl methacrylate) (T-PBMA) and poly(vinylbenzyladenine-co-styrene) (A-PS)

The solution copolymerizations of butyl methacrylate and VBT and of styrene and VBA were performed in DMF at 70 °C under an argon atmosphere within glass reaction flasks equipped with condensers. AIBN was employed as the initiator; the mixtures were stirred for ca. 24 h. The products were dissolved in DMF and then poured into excess methanol under vigorous agitation to precipitate the copolymers. T-PBMA and A-PS were characterized using ^{1}H nuclear magnetic resonance (NMR) spectroscopy, Fourier transform infrared (FTIR) spectroscopy, differential scanning calorimetry (DSC), thermogravimetric analysis (TGA), and gel permeation chromatography (GPC). To determine the reactivity ratios, samples of the copolymers were taken from the reaction flasks during the early stages of copolymerization, i.e., when the degrees of conversion were low (4–9%). Scheme 2 outlines the synthetic procedures and the structures of the various components.

2.2. Blend preparation

Blends of A-PS and T-PBMA were prepared through solution-blending. THF solutions containing 5 wt% of the polymer mixture were stirred for 6–8 h; the solvent was then left to evaporate slowly at room temperature for 24 h. The blend films were then dried at 50 °C for 2 days.

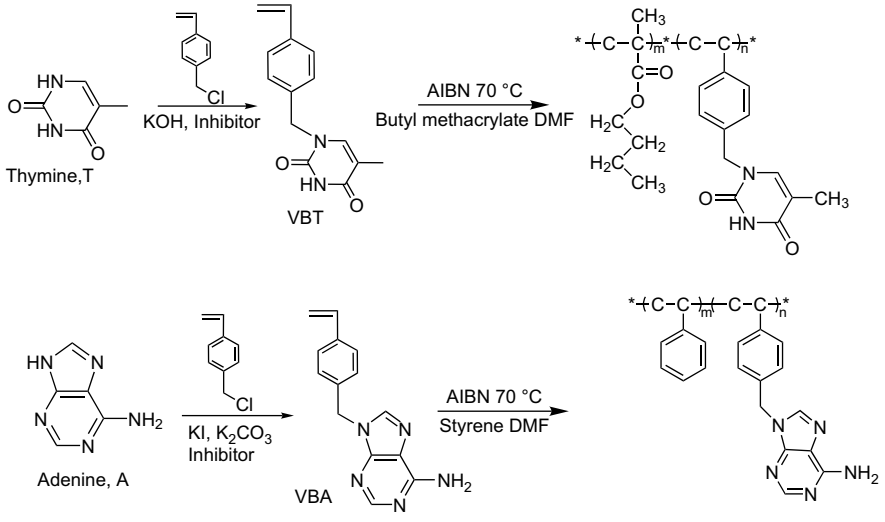

Scheme 2. Syntheses of A-PS and T-PBMA random copolymers through free radical polymerization.

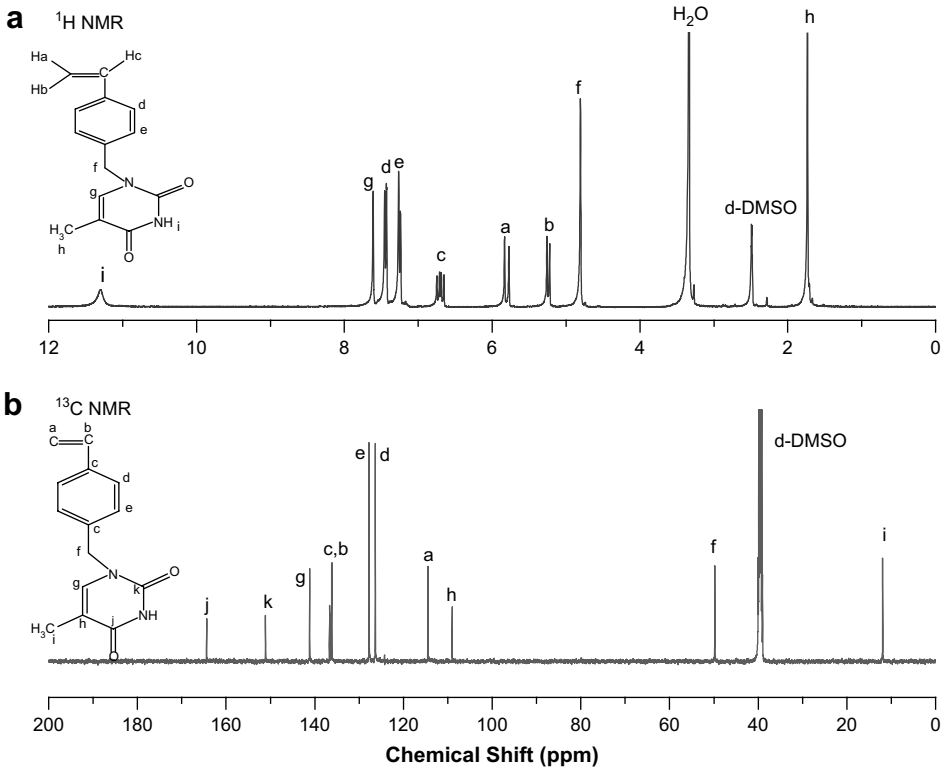

Fig. 1. ^{1}H and ^{13}C NMR spectra of VBT in d_6-DMSO at room temperature.

2.3. Characterization

Molecular weights and molecular-weight distributions were determined at 40 °C through GPC using a Waters 510 HPLC equipped with a 410 differential refractometer, an UV detector, and three Ultrastyragel columns (100, 500, and 10^3 Å) connected in series; THF was the eluent; the flow rate was 0.6 mL/min. The molecular-weight calibration curve was obtained using PS

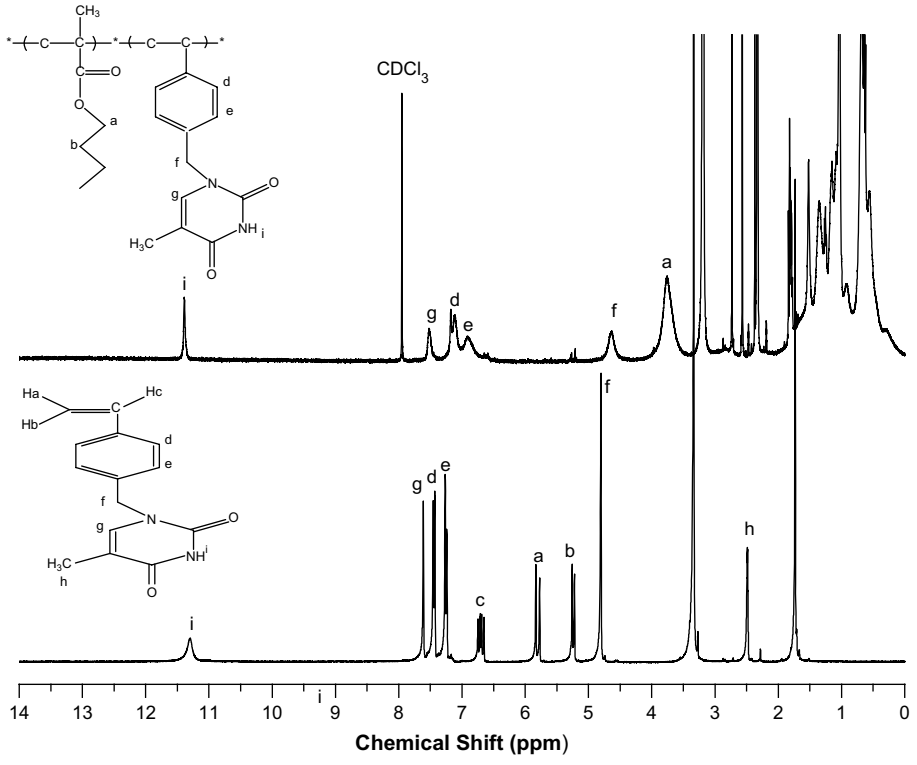

Fig. 2. ^{1}H NMR spectra of VBT and T-PBMA copolymers in d_6-DMSO at room temperature.

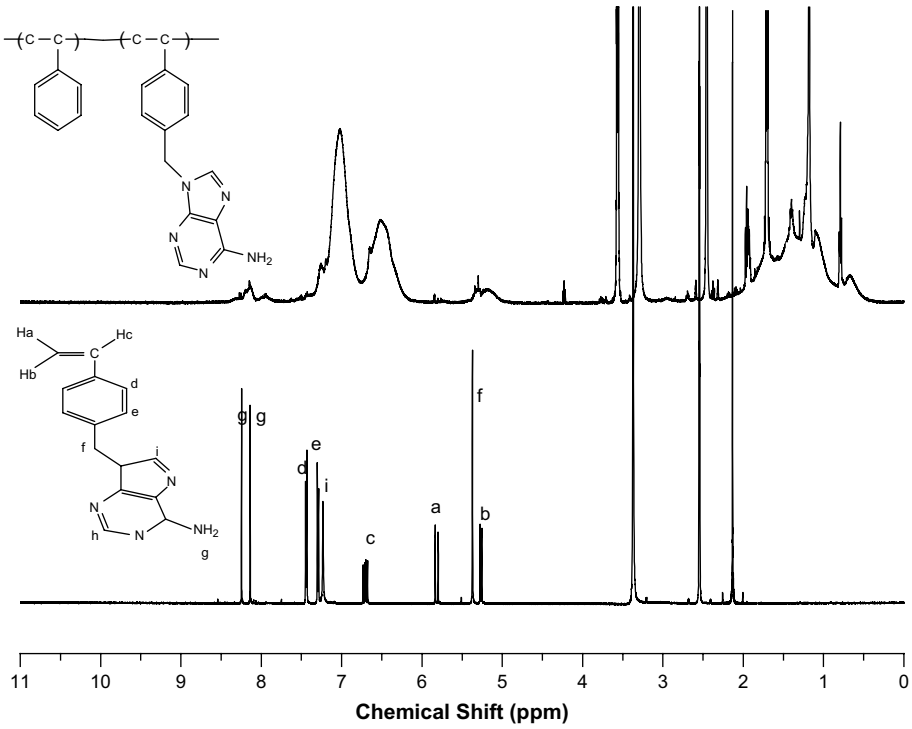

Fig. 3. ^{1}H NMR spectra of VBA and A-PS copolymers in d_6-DMSO at room temperature.

standards. ^{1}H and ^{13}C NMR spectra were obtained using an INOVA 500 instrument; acetone-d_6 was the solvent. The spectra were measured with a 3.9 μs 90° pulse, with 3 s pulse delay time, acquisition time of 30 ms and 2048 scans were accumulated. The glass transition temperatures (T_gs) of the polymer blend films were determined through DSC using a TA Q-20 instrument. The scan rate was 20 °C/min within the temperature range 30–200 °C; the temperature was then held at 200 °C for 3 min to ensure complete removal of the residual solvent. The T_g measurements were performed in the DSC sample cell after the sample (5–10 mg) had been cooled rapidly to −50 °C from the melt of the first scan. The glass transition temperature was defined as the midpoint of the heat capacity transition between the upper and lower points of deviation from the extrapolated liquid and glass lines. TGA was performed under nitrogen or air using a TA Q50 thermogravimetric analyzer operated at a heating rate of 20 °C/min over the temperature range from room temperature to 800 °C. The rate of nitrogen or air flow was 60 mL/min. FTIR spectra of the polymer blend films were recorded using the conventional KBr disk method. A THF solution containing the blend was cast onto a KBr disk and dried under conditions similar to those used in the bulk preparation. The film used in this study was sufficiently thin to obey the Beer–Lambert law. FTIR spectra were recorded using a Bruker Tensor 27 FTIR spectrophotometer; 32 scans were collected at a spectral resolution 1 cm^{-1}. Because polymers containing A and T groups are hygroscopic, pure nitrogen gas was used to purge the spectrometer's optical box to maintain the sample films' dryness. Generalized 2D correlation analysis was performed using the 2D Shige software developed by Shigeaki Morita (Kwansei-Gakuin University, Japan). In the 2D correlation maps, white-colored regions are defined as positive correlation intensities; shaded regions are defined as negative correlation intensities. The hydrodynamic diameters of the assemblies were measured through dynamic light scattering (DLS) using a Brookhaven 90 plus instrument (Brookhaven Instruments, USA) equipped with a He–Ne laser operated at a power of 35 mW at 632.8 nm. All DLS measurements were performed using a wavelength of 632.8 nm at 25 °C and an angle of 90°.

Table 1
Properties of the A-PS and T-PBMA poly(VBT-*co*-PBMA) and poly(VBA-*co*-PS) copolymers.

Sample	Feed	Copolymer[a]	M_w[b]	M_n[b]	PDI[b]	T_g[c] (°C)	T_d[d] (°C)
	VBT/BMA	PVBT/PBMA					
Pure PBMA	0:100	0	42 000	25 000	1.68	31.4	325.9
T7-PBMA93	4:96	7:93	41 000	24 700	1.65	40.4	336.8
T11-PBMA89	6:94	11:89	45 200	28 700	1.57	49.0	346.6
T24-PBMA76	13:87	24:76	49 600	32 900	1.50	61.0	381.6
	VBA/styrene	PVBA/PS					
Pure PS	0:100	0	25 400	17 000	1.50	90.2	401.2
A05-PS95	2:98	5:95	25 800	17 100	1.50	106.7	413.7
A08-PS92	4:96	8:92	33 100	17 400	1.90	112.0	413.9
A11-PS89	9:91	11:89	32 200	17 600	1.82	114.0	415.8

[a] Estimated from ^{1}H NMR.
[b] Relative molecular weights against polystyrene standard calculated from GPC in THF.
[c] Determined by DSC at 20 °C/min.
[d] Determined by TGA at 20 °C/min.

3. Results and discussion

3.1. Analyses of monomers and copolymers

VBT and VBA are soluble in most common solvents. Fig. 1 shows ^{1}H and ^{13}C NMR spectra of VBT in d_6-DMSO solvent. For the VBT, two doublets and the quartet resonance proton resonance peaks from the vinyl group (1$\mathbf{H}_b$, 1$\mathbf{H}_a$ and 2$\mathbf{H}_c$) in the VBT are located at 5.26, 5.77 and 6.98 ppm with relative mole ratio of 1:1:1, corresponding to iso-, trans- and substituted vinyl protons. The resonances of methyl in thymine ($\mathbf{H}_h$), and benzyl CH_2 ($\mathbf{H}_f$) at a mole ratio of 3:2 are observed at $\delta = 1.80$ and 4.87 ppm, respectively. The NH in thymine group is located at 11.30 ppm and all other peaks are assigned as shown in Fig. 1(a). Fig. 1(b) displays the corresponding

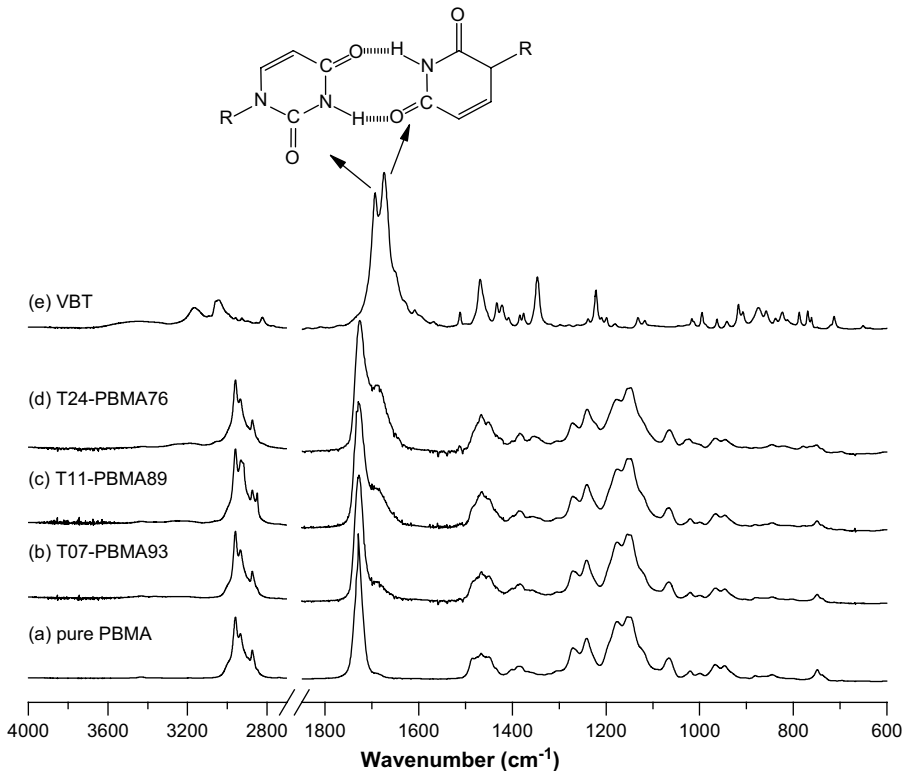

Fig. 4. FTIR spectra of VBT and T-PBMA copolymers at room temperature.

^{13}C NMR spectra of the VBT. All peaks are assigned as shown in Fig. 1(b), indicating that the synthesis of VBT monomer is successful. Fig. 2 compares the ^{1}H NMR spectra of VBT and T24-PBMA (i.e., the T-PBMA copolymer containing 24 mol% of VBT). The signals of the vinylic hydrogen atoms of VBT are absent in the spectrum of T24-PBMA, indicating that the starting monomers were completely removed. We estimated the mole percentage of VBT from the ratio of the integrals of benzylic ($\mathbf{H}_f$) protons of VBT and the OCH_2 ($\mathbf{H}_a$) protons of BMA.

Fig. 3 compares the ^{1}H NMR spectra of VBA and A11-PS (11 mol% VBA). Again, the signals for the vinylic hydrogen atoms of VBA are absent in the spectrum of the A11-PS copolymer. We estimated the mole percentage of VBA in the A-PS copolymer from the ratio of the integrals of the aromatic protons of the PS units (6.5–7.5 ppm) and the benzylic protons of the VBA units. Table 1 lists the monomer feed ratios and resultant copolymer compositions from which we calculated the reactivity ratios ($r_{VBT} = 3.92$ and $r_{BMA} = 0.60$; $r_{VBA} = 4.60$ and $r_{St} = 0.33$) using the methodology of Kelen and Tudos, as discussed in previous study [13,31]. The apparent linear relationship suggests that the copolymerization of these two co-monomers followed a simple two-parameter (terminal) model [32]. The products of the reactivity ratios were within the range 1.5–2.4 which indicates that these two monomers were introduced into the polymer chain in an essentially random manner with only a slight tendency toward blocky. Hence, these copolymers synthesized by free radical polymerization are essentially random copolymers.

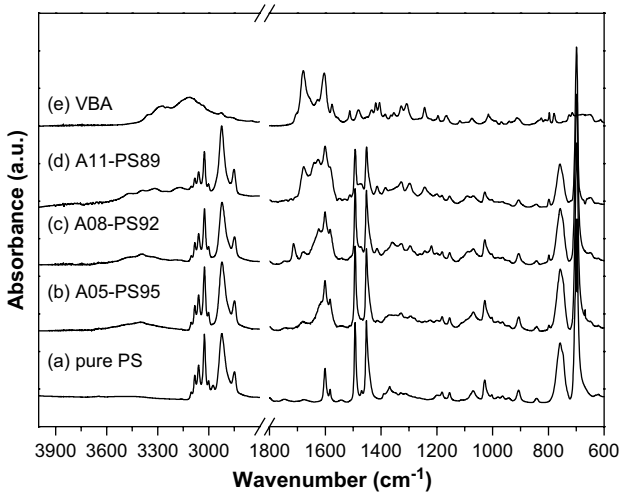

Fig. 5. FTIR spectra of VBA and A-PS copolymers at room temperature.

Fig. 4 displays FTIR spectra of VBT and the T-PBMA copolymers at room temperature. For pure VBT, bands appear at 3440 (free NH stretching), 3168 (hydrogen-bonded NH stretching), 3044 (vinyl CH stretching), and 2800 cm^{-1} (CH stretching). Two strong bands at 1694 and 1674 cm^{-1} correspond to free and hydrogen-bonded C=O groups, respectively, as indicated in the inset [22]. For the T-PBMA copolymers, the signal for the vinyl group at 3044 cm^{-1} is absent, consistent with the formation of random T-PBMA copolymers. The signal of the free C=O groups of PBMA appears at 1730 cm^{-1}; the intensity of the absorption of the thymine C=O group at ca. 1688 cm^{-1} increased upon increasing the VBT fraction in the copolymers. Because the thymine groups were distributed randomly in the PBMA, the probability of self-associative hydrogen bonding of thymine group was low; thus, the shift in the absorption from 1674 to 1688 cm^{-1} was due to the diluent effect in the hydrogen bonding system [33,34].

Fig. 5 displays FTIR spectra of VBA and the A-PS copolymers at room temperature. For VBA, bands appear at 3363 (free NH_2

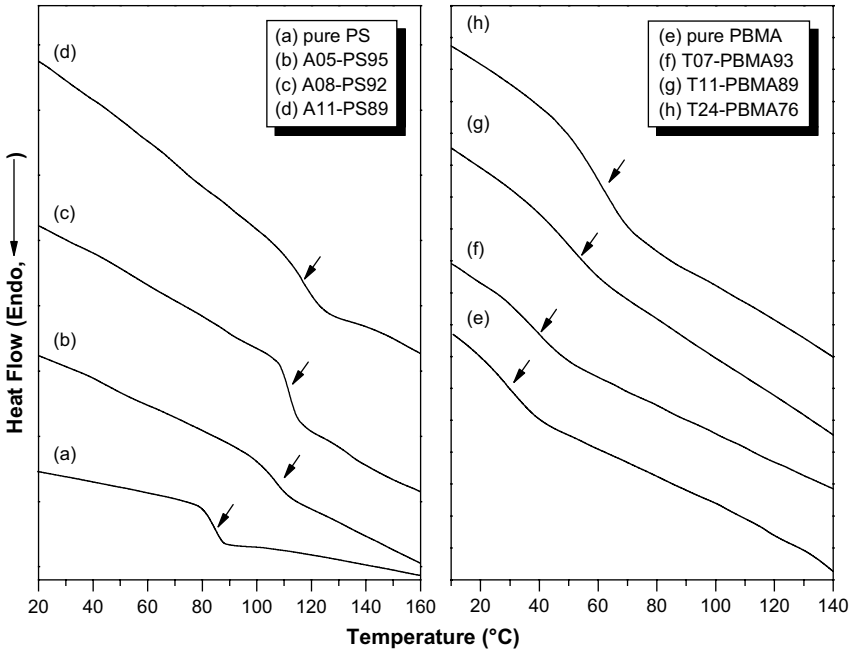

Fig. 6. DSC thermograms of A-PS and T-PBMA copolymers.

stretching), 3282 (hydrogen-bonded NH stretching), 3118 (vinyl and aromatic CH stretching), and 2930 cm^{-1} (benzylic CH_2 stretching). The two strong bands at 1675 and 1602 cm^{-1} correspond to bonded NH_2 scissor plus ring stretching and ring stretching plus bonded NH_2 scissor, respectively. The small bands at 1630 and 1575 cm^{-1} correspond to free NH_2 scissor plus ring stretching and ring stretching plus ring stretching [22]. For the A-PS copolymers, the intensity of the signals for the adenine group increased upon increasing the VBA fraction in the copolymer, but the signal of the vinyl group at 3188 cm^{-1} was absent, consistent with the formation of random A-PS copolymers. Similar to the phenomenon in the spectra of the T-PBMA copolymers, the signals of the adenine units in the A-PS copolymers all shifted to higher wavenumber due to the diluent effect of the styrene segments [33].

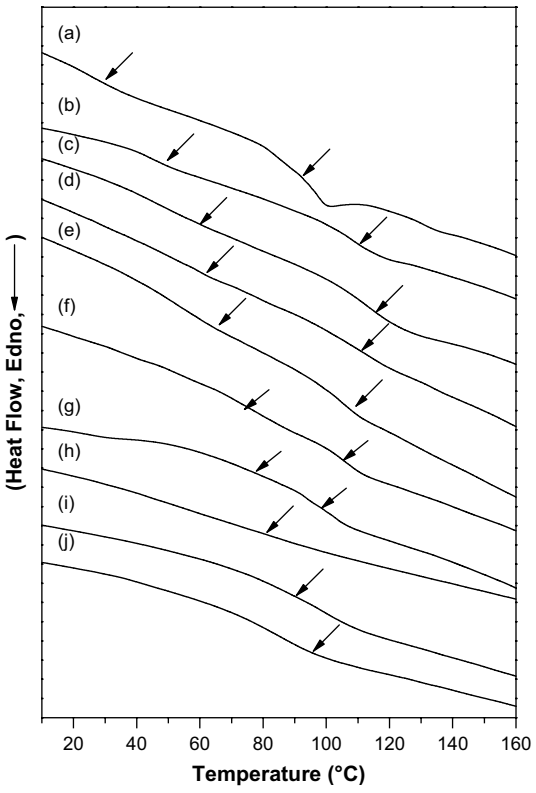

Fig. 7. DSC curves of the binary blends (a) PS/PBMA, (b) A5-PS/T7-PBMA, (c) A5-PS/T11-PBMA, (d) A5-PS/T24-PBMA, (e) A8-PS/T7-PBMA, (f) A8-PS/T11-PBMA, (g) A11-PS/T7-PBMA, (h) A8-PS/T11-PBMA, (i) A11-PS/T11-PBMA, and (j) A11-PS/T24-PBMA.

Fig. 6 displays DSC curves, recorded from 10 to 160 °C, of the A-PS and T-PBMA copolymers. The glass transition temperature of these two copolymers increased upon increasing the contents of A and T units, with the Fox equation revealing a positive deviation [35]. In addition, the thermal decomposition temperatures also increased significantly upon increasing the contents of these nucleobases. Table 1 summarizes the monomer feed ratios and the compositions, molecular weights, glass transition temperatures, and thermal decomposition temperatures of the synthesized copolymers. In terms of nomenclature, the descriptor T7-PBMA93, for example, represents a copolymer containing 7 mol% of VBT.

3.2. Analyses of A-PS/T-PBMA binary blends

3.2.1. Morphology and DSC analyses

A single value of T_g detected by DSC is conventionally employed as a criterion reflecting the miscibility of a polymer blend. A single

Table 2
Summary data from the DSC analysis of A-PS/T-PBMA binary blends.

Sample (corresponding T_g)	T_g		Fox rule predicted
PS/PBMA (90/31)	87	31	
A05-PS/T7-PBMA (107/40)	108	43	
A05-PS/T11-PBMA (107/49)	104	53	
A05-PS/T24-PBMA (107/61)	108	60	
A08-PS/T7-PBMA (112/40)	112	46	
A08-PS/T11-PBMA (112/49)	94	78	
A11-PS/T7-PBMA (114/40)	114	60	
A11-PS/T11-PBMA (114/49)	73		68
A08-PS/T24-PBMA (112/61)	86		79
A11-PS/T24-PBMA (114/60)	99		80

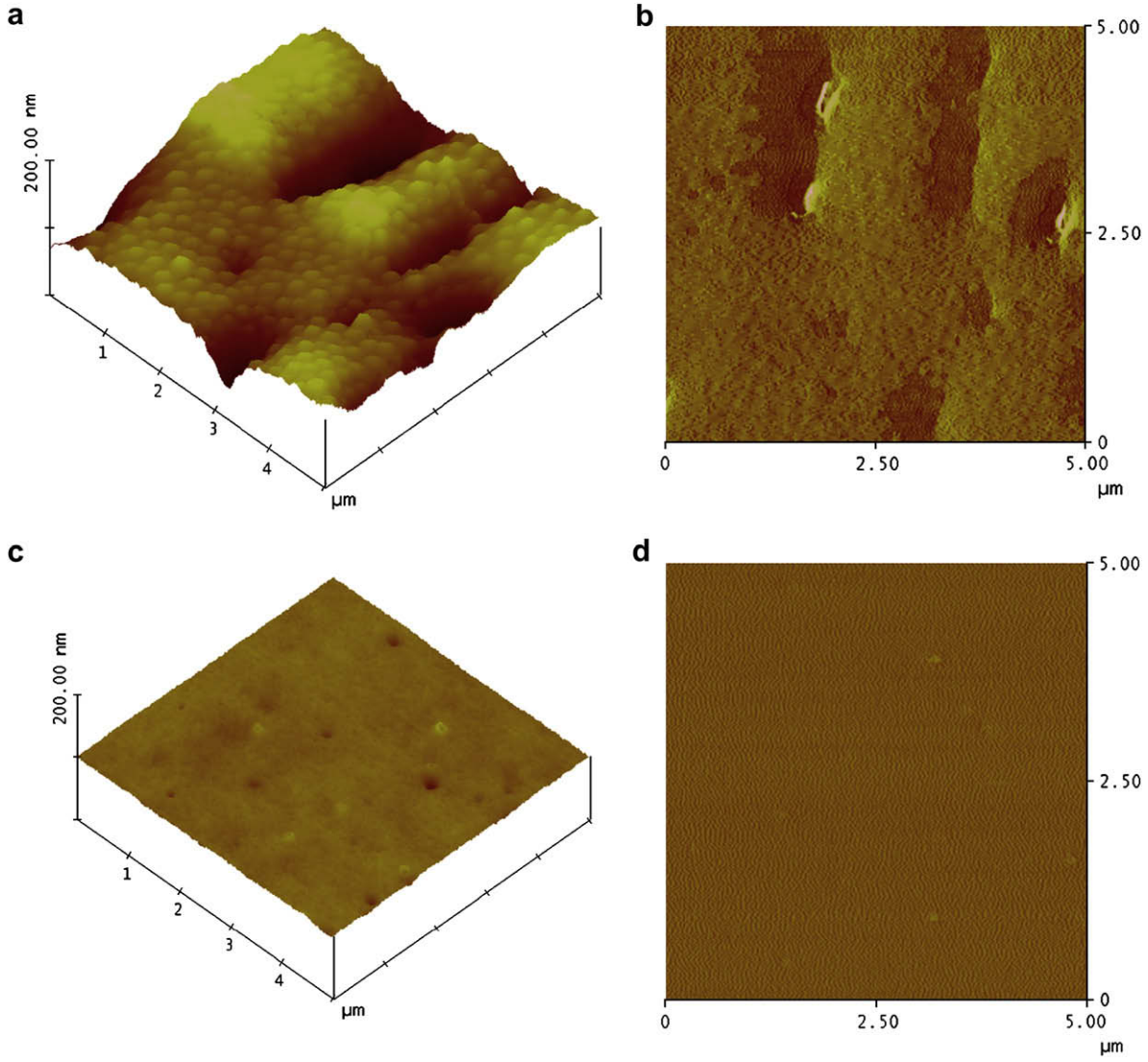

Fig. 8. Tapping mode AFM images of PS/PBMA blend: (a) height and (b) phase images, and A11-PS/T24-PBMA blend: (c) height and (d) phase images.

compositionally dependent glass transition implies full miscibility of the blend at dimensions on the order of 20–40 nm. Fig. 7 displays DSC thermograms of A-PS/T-PBMA = 50/50 blends, where the A-PS and T-PBMA components contain various contents of VBA and VBT, respectively; Table 2 summarizes the data. The binary blend of PS and PBMA exhibits two glass transition temperatures located at the same temperatures as those of their respective pure polymers, revealing that they are completely immiscible. We found, however, that the value of T_g shifted upon increasing the VBA and VBT contents in the copolymers; when 8 mol% or more of VBA and 11 mol% or more of VBT were incorporated into the PS and PBMA main chains, respectively, the PS/PBMA binary blends formed miscible pairs exhibiting a single value of T_g through strong multiple hydrogen bonding interactions between the A and T units. Meanwhile, the single values of T_g of the copolymer blends fall between those of the two parent polymers (PS and PBMA), but they are significantly higher than the values predicted by the Fox equation, again indicating the presence of strong multiple hydrogen bonding interactions between the A and T segments in the copolymers.

According to the PCAM [24], two major factors are responsible for an increase in the miscibility window. First, when the difference in the solubility parameters of the two blend components is low, the corresponding value of χ will also be low. Secondly, the strength of inter-association over self-association will increase upon increasing the VBA and VBT contents in the copolymers; this phenomenon tends to enhance the favorable contribution from the $\Delta G_H/RT$ term in the PCAM and, therefore, improves the miscibility. We discuss in a later section the optimal values of the VBA and VBT contents in the PS and PBMA copolymers that provide the most favorable miscible blends.

In addition, Fig. 8 shows AFM images for providing microscopic evidence for the homogeneous mixing without phase separation. The thin film prepared by casting a 4.0 g/dL solution of PBMA and PS in chloroform on glass exhibited islands with lateral dimensions ca. 100 nm (Fig. 8(a) and (b)). However, the thin film of a mixture of A11-PS and T24-PBMA prepared in the same way as that above was smooth, with no features evident on the nanometer scale (Fig. 8(c) and (d)). These observations are consistent with the formation of a miscible blend driven by the A–T recognition. Although the structure of the polymer assembly is not known, it is likely that a supramolecular network is formed.

3.2.2. FTIR spectroscopic analyses

Infrared spectroscopy is a highly effective means of investigating the specific interactions between polymers. It can be used as a tool

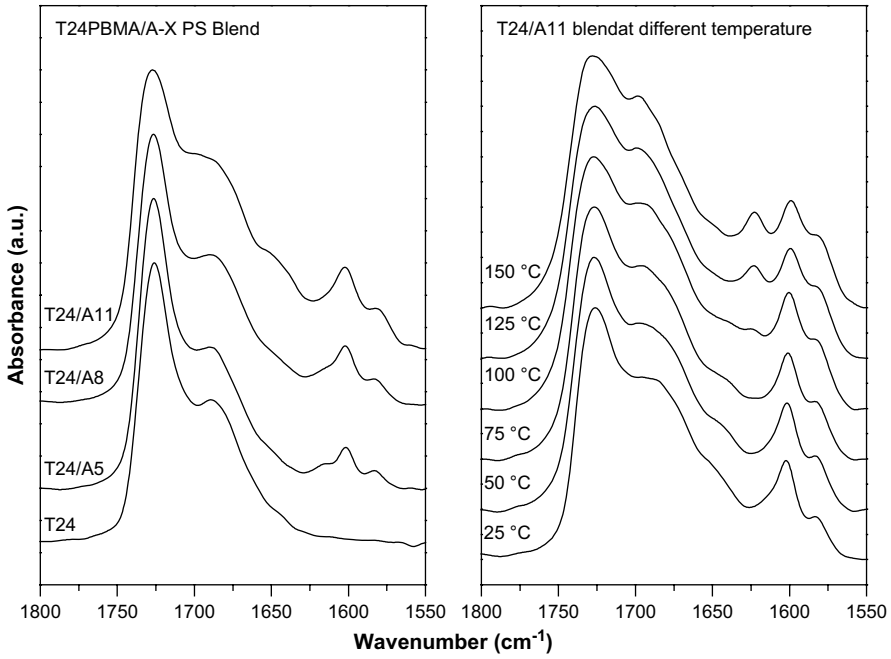

Fig. 9. FTIR spectra of (a) T24-PBMA/A-PS blends featuring various A contents recorded at room temperature and (b) the T24-PBMA/A8-PS blend at various temperatures.

to study, both qualitatively and quantitatively, the mechanism of inter-polymer miscibility through the formation of hydrogen bonds. Fig. 9 displays FTIR spectra (1550–1800 cm^{-1}) recorded at room temperature for T24-PBMA blended with A-PS copolymers containing various mole percentages of A units, as well as spectra of the T24-PBMA/A8-PS = 50/50 blend at various temperatures. As mentioned above, the signal of the free C═O groups of PBMA appears at 1730 cm^{-1} and the absorption at ca. 1688 cm^{-1} is due to the thymine groups [Fig. 9(a)]. Clearly, the position of signal for the free C═O groups of PBMA did not change upon increasing the content of A units, implying that the A did not form the hydrogen bonding with carbonyl group of PBMA. We did, however, observe a new peak at ca. 1650 cm^{-1}, corresponding to multiple hydrogen bonding interactions between the T and A groups, that grew upon increasing the content of the A units; the intensity of this peak decreased upon increasing the temperature [Fig. 9(b)] because heat disrupts hydrogen bonding interactions. At temperatures higher than the value of T_g of the T24-PBMA/A8-PS blend, a new peak appeared at ca. 1630 cm^{-1} corresponding to free NH_2 scissor plus ring stretching, indicating that the multiple hydrogen bonding interactions between the A and T groups were disrupted.

We used two-dimensional correlation spectroscopy to further characterize the interactions in this blend system. 2D correlation spectroscopy has recently been applied widely in polymer science [36–40] as a novel method that allows the specific interactions between polymer chains to be investigated by treating the spectral fluctuations as a function of time, temperature, pressure, and composition. 2D IR correlation spectroscopy can identify various intra- and intermolecular interactions through analysis of selected bands from the 1D vibration spectrum. White and shaded areas in 2D IR correlation contour maps represent positive and negative cross-peaks, respectively. In general, two types of spectra, 2D

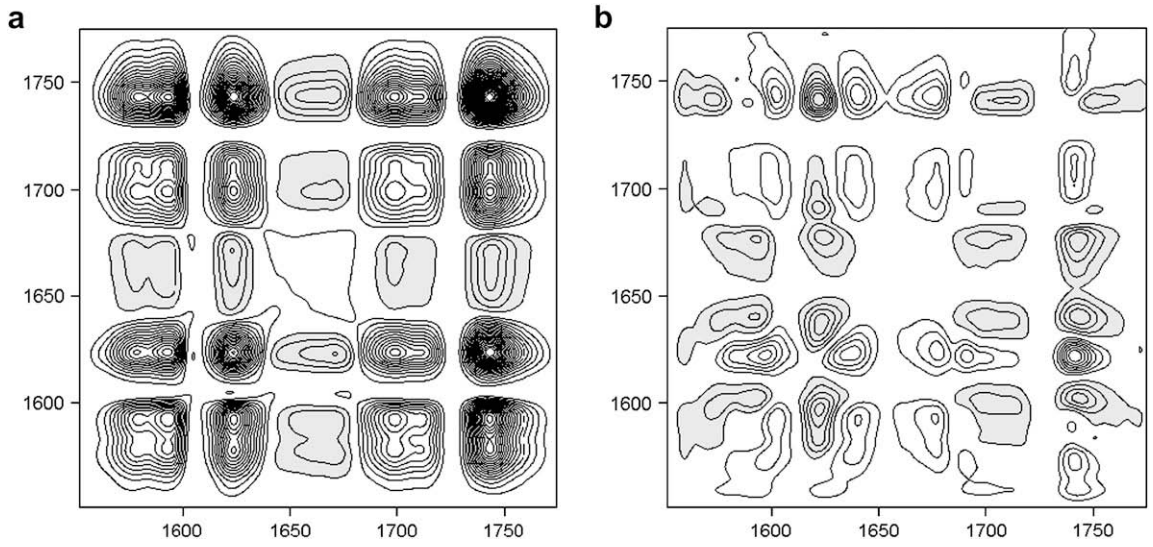

Fig. 10. (a) Synchronous and (b) asynchronous 2D IR correlation maps (1550–1800 cm^{-1}) for A-PS/T-PBMA blends under temperature perturbation.

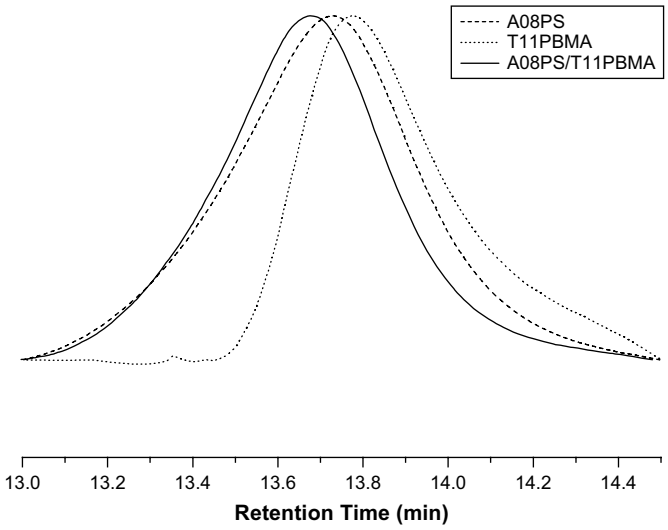

Fig. 11. SEC traces of A8-PS, T11-PBMA, and the A8-PS/T11-PBMA blend in THF solution.

synchronous and asynchronous, are obtained; the correlation intensities in the 2D synchronous and asynchronous maps reflect the relative degrees of in-phase and out-of-phase responses, respectively. The 2D synchronous spectra are symmetric with respect to the diagonal line in the correlation map. Auto peaks, which represent the degree of autocorrelation of perturbation-induced molecular vibrations, are located at the diagonal positions of a synchronous 2D spectrum; their values are always positive. When an auto peak appears, the signal at that wavenumber would change greatly under environmental perturbation. Cross-peaks located at off-diagonal positions of a synchronous 2D spectrum (they may be positive or negative) represent the simultaneous or coincidental changes of the spectral intensity variations measured at ν_1 and ν_2. Positive cross-peaks result when the intensity variations of the two peaks at ν_1 and ν_2 occur in the same direction (i.e., both increase or both decrease) under the environmental perturbation; negative cross-peaks reveal that the intensities of the two peaks at ν_1 and ν_2 change in opposite directions (i.e., one increases while the other decreases) under perturbation [41].

As in the case for a synchronous spectrum, the sign of an asynchronous cross-peak can be either negative or positive, providing useful information on the sequential order of events observed by the spectroscopic technique along the external variable. The 2D asynchronous spectra are asymmetric with respect to the diagonal line in the correlation map. According to Noda's rule [38], for $\Phi(\nu_1,\nu_2) > 0$, if $\psi(\nu_1,\nu_2)$ is positive (black colored area), band ν_1 will vary prior to band ν_2; if $\psi(\nu_1,\nu_2)$ is negative (white-colored area), band ν_2 will vary prior to band ν_1. This rule is reversed, however, for $\Phi(\nu_1,\nu_2) < 0$. In summary, if the symbols of the cross-peak in the synchronous and asynchronous maps are the same (both positive or both negative), band ν_1 will vary prior to band ν_2; if the symbols of the cross-peak are different in the synchronous and asynchronous spectra (one positive and the other negative), band ν_1 will vary after ν_2 under the environmental perturbation.

Fig. 10(a) presents the synchronous 2D IR correlation maps in the range 1550–1800 cm^{-1}. Absorption bands in this spectral range that are associated with T-PBMA appear at 1740 cm^{-1} (free C═O groups of PMBA) and ca. 1694 cm^{-1} (free C═O groups of T units). The signals associated with A-PS appear at 1630 and 1575 cm^{-1} for free NH_2 units and at 1675 and 1602 cm^{-1} for hydrogen-bonded NH_2 groups. Six positive cross-peaks existed for this system: (1575 vs 1630), (1575 vs 1694), (1575 vs 1740), (1630 vs 1694), (1630 vs 1740), and (1688 vs 1730). These positive cross-peaks all exhibit the same direction (according to Noda's rule) upon increasing the temperature because all these peaks correspond to free functional groups. The signal at 1675 cm^{-1} had four negative cross-peaks with those at 1575, 1630, 1694, and 1740 cm^{-1}, indicating that these latter four bands vary in the opposite direction to that at 1650 cm^{-1}. Undoubtedly, these four free functional groups should vary in opposite direction with the hydrogen-bonded functional group.

Fig. 10(b) displays the asynchronous 2D correlation maps in the range 1550–1800 cm^{-1}. The cross-peaks between the signal at 1675 cm^{-1} and those at 1575, 1630, and 1694 cm^{-1} exhibit opposing intensity orders, indicating that these bands result from different polymer chains, i.e., intermolecular multiple hydrogen bonding between A and T groups. In addition, the positive peaks at (1740, 1694 cm^{-1}), (1694, 1575 cm^{-1}), (1575, 1630 cm^{-1}), and (1630, 1675) in the asynchronous map imply that, upon increasing the temperature, the intensity of the peak at 1740 cm^{-1} alters before that at 1694 cm^{-1}, 1694 cm^{-1} alters before that at 1575 cm^{-1}, 1575 cm^{-1} alters before that at 1630 cm^{-1}, and 1630 cm^{-1} alters before that at 1675 cm^{-1}. Taken together, the 2D map reveals that,

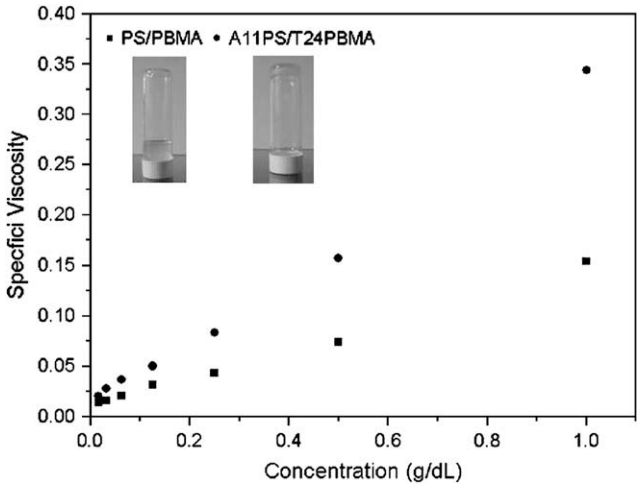

Fig. 12. Plots of specific viscosity of PS/PBMA and A11-PS/T24-PBMA blends in THF solution with respect to concentration. Inset: Photographs of the corresponding blends at a concentration of 30 g/dL.

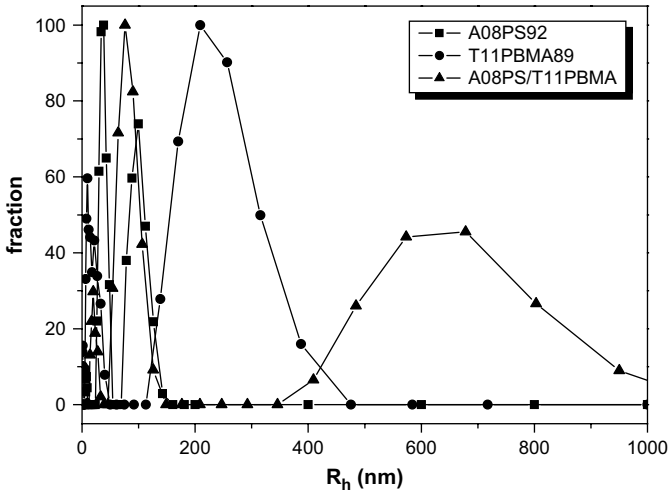

Fig. 13. DLS analysis of A8-PS, T11-PBMA, and the A8-PS/T11-PBMA blend in THF solution.

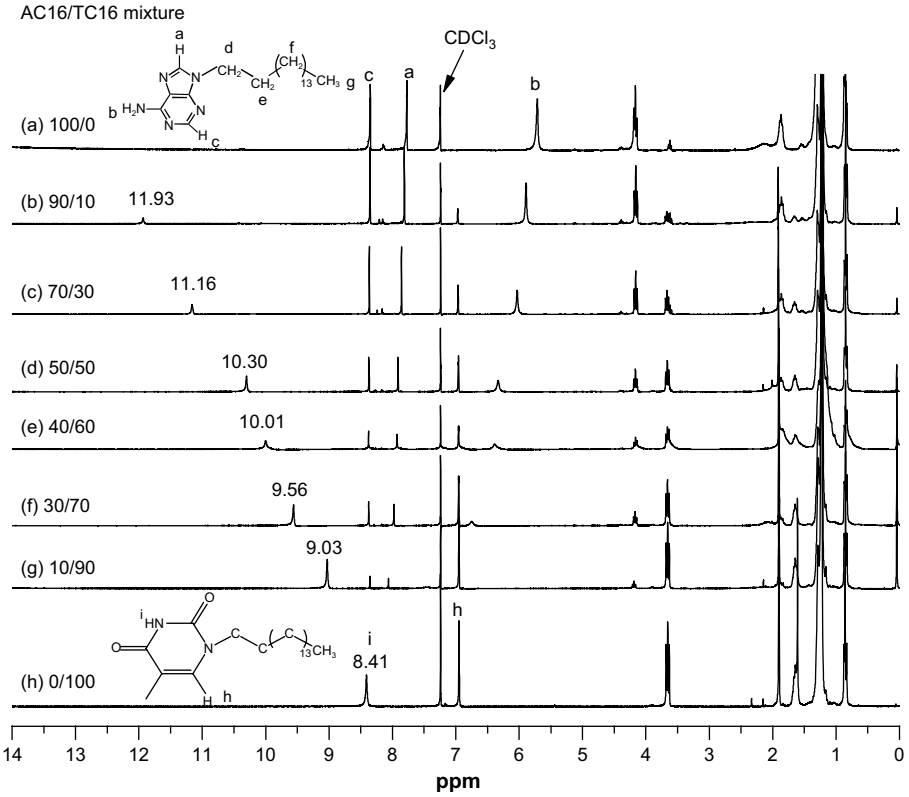

Fig. 14. ^{1}H NMR spectra ($CDCl_3$, room temperature) of A-16/T-16 mixtures featuring various A/T ratios.

upon increasing the temperature, the sequence of changing intensity of the three bands observed in the spectra was $1740 > 1694 > 1575 > 1630 > 1675\ cm^{-1}$. This result is reasonable because the presence of multiple hydrogen bonding interactions is more favorable than having free C═O and NH_2 groups and results in the last influence with the increase of temperature.

3.2.3. SEC, viscosity, and DLS analyses of supramolecular structure

We used size exclusion chromatography (SEC) with UV detection at 245 nm to examine the aggregation of A-PS and T-PBMA in THF solution. SEC, also known as GPC, is an analytical technique in which the separation of components in a reaction mixture is based on their size, rather than their chemical affinity to the stationary phase. GPC has been used extensively for the determination of polymer dispersity and molecular weight, as well as in the analysis of large biomolecules such as proteins. Using GPC for supramolecular characterization can, in principle, greatly facilitate the analysis of the relative size and stability of several similar hydrogen-bonded supramolecular aggregates [42,43]. Fig. 11 reveals that the retention time for the binary A8-PS/T11-PBMA blend decreased relative to those of its individual pure copolymers, indicating that aggregates of large size—supramolecular polymers—had formed through multiple hydrogen bonding interactions between the A units of PS and the T units of the PBMA chains. We further characterized the blends by using a Ubbelohde viscometer to measure the solution viscosity of a mixture of A-PS and T-PBMA in THF (Fig. 12). The formation of supramolecular polymers in the A-PS/T-PBMA blends led to higher solution viscosity than that of the PS/PBMA blend; in addition, the viscosity increased upon increasing the concentrations of the copolymers. This supramolecular polymer also could be observed macroscopically from a 1:1 mixture of A11-PS/T24-PBMA in THF at a concentration of 30 g/dL, which formed a gel; at the same concentration, a solution of PBMA and PS, which lacked any

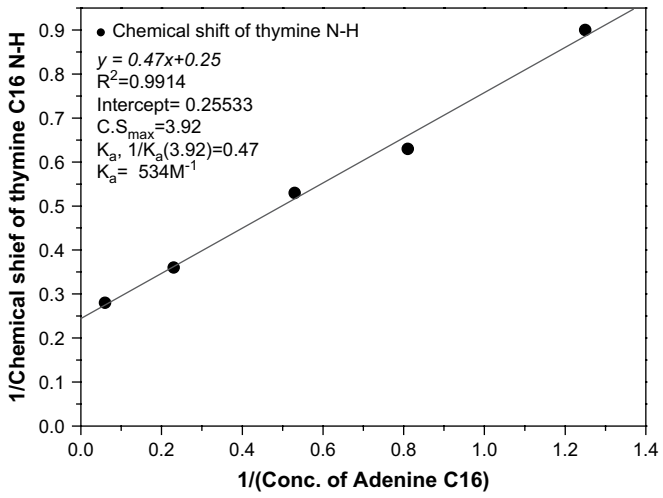

Fig. 15. Determination of the inter-association equilibrium constant for the A···T interaction using the Benesi–Hildebrand method.

Table 3
Summary of the self- and inter-association equilibrium constants, and their thermodynamic parameter of A-PS/T-PBMA blends at 25 °C.

Polymer	Molar volume (ml/mol)	Molecular weight (g/mol)	δ (cal/ml)$^{1/2}$	Equilibrium constant	
				K_B	K_A
PS	93.9	104.1	9.5		
PBMA	134.4	142	8.7		
PVBA	112.5	251.1	13.2	32.0	
PVBT	161.7	242.1	12.1		4750

δ: Solubility parameter, K_B: self-association equilibrium constant, K_A: Inter-association equilibrium constant.

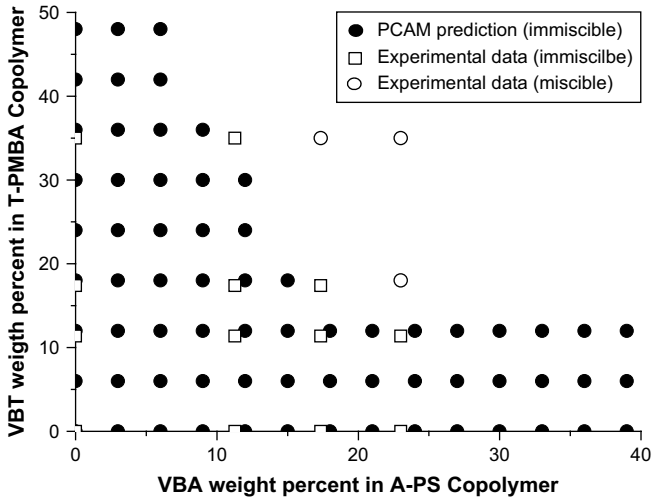

Fig. 16. Theoretical miscibility windows for A-PS/T-PBMA blends obtained from the PCAM; (●) spinodal curve and experimental data; (□) two-phase system; (○) one-phase system.

specific inter-polymer hydrogen bonding interactions, flowed freely (see the inset of Fig. 12). We also used DLS to characterize the supramolecular structures formed from the A-PS/T-PBMA mixtures in THF. We analyzed the experimental correlation function using the cumulant method and the CONTIN algorithm, as described previously [44]. The Stokes–Einstein approximation was used to convert the diffusion coefficient into the form of the hydrodynamic diameter (D_h). Fig. 13 reveals that the dependence of the hydrogen bonding interaction on the A-PS/T-PBMA mixture was complicated; for the A8-PS/T11-PBMA blend at molar ratio of 1:1, the largest peak associated with polymer aggregates appeared as a broad signal at ca. 650 nm, providing direct evidence for hydrogen bond-mediated aggregate formation.

3.2.4. PCAM analysis of miscibility window

Painter and Coleman [27] suggested adding an additional term—accounting for the free energy of hydrogen bond formation—to a simple Flory–Huggins expression for the free energy of mixing of two polymers:

$$\frac{\Delta G_N}{RT} = \frac{\Phi_1}{N_1}\ln \Phi_1 + \frac{\Phi_2}{N_2}\ln \Phi_2 + \Phi_1\Phi_2\chi_{12} + \frac{\Delta G_H}{RT} \quad (1)$$

where Φ and N are the volume fraction and the degree of polymerization, respectively, χ is the "physical" interaction parameter, and the subscripts 1 and 2 define the two blend components; ΔG_H is the free energy change contributed by hydrogen bonding between two components. According to the Painter–Coleman equation, the relative magnitude of the inter- and self-association equilibrium constants, rather than their individual absolute values, is the most important factor when determining the dominant contributions to the free energy of mixing. In general, the inter-association equilibrium constant K_A is calculated using one of the two methods: either from the polymer blend system or from a low-molecular-weight model compound [45]. In our system, pure PVBA and PVBT dissolve only in high-polarity solvents, such as DMF and DMSO, which interfere with self- and inter-association hydrogen bonding and would, therefore, provide incorrect equilibrium constants [27]. Thus, we synthesized two low-molecular-weight model compounds, 9-hexadecyladenine (AC-16) and 9-hexadecylthymine (TC-16), to determine the inter-association equilibrium constants (K_a) through ^{1}H NMR spectroscopic titration experiments in $CDCl_3$ at room temperature, based on the method developed by Benesi and Hildebrand [46].

Fig. 14 displays ^{1}H NMR spectra of AC-16/TC-16 mixtures at various ratios. The addition of AC-16 to a TC-16 solution led to a downfield shift of the signal of the thymine group that appeared initially at 8.41 ppm, indicating that strong intermolecular hydrogen bonding occurred between the T and A groups. A plot of this chemical shift vs the reciprocal of the concentration (Fig. 15) allowed us to calculate the inter-association equilibrium constant ($K_a = 534\ M^{-1}$). We transformed the value of K_a from the model compound into K_A by dividing by the molar volume of the VBA repeat unit (0.1125 L mol^{-1} at 25 °C) [24], providing a value for the inter-association equilibrium constant K_A of 4750. Likewise, we determined that the self-association equilibrium constant (K_B) of adenine was 32, after dividing the value of K_b of 3 M^{-1} for the model compound 2-ethyladenine by the molar volume of the VBA repeat unit [22]. To minimize errors, we ignored the self-association of T groups because the T–T interaction is almost the same strength as the A–A interaction [22]; furthermore, two self-associating, hydrogen-bonded donor polymer blend systems would make analysis of the binary blend system too complicated [47,48].

Although we did not obtain these inter-association equilibrium constants from polymer mixtures, the standard inter-association equilibrium constant of the polymer blend could be calculated from the low-molecular-weight model compound mixtures based on considering the intramolecular screening effect and functional group accessibility [24]. The intramolecular screening effect is a consequence of chain connectivity. The covalent linkage between polymer segments causes an increase in the number of same-polymer-chain contacts as a result of the polymer chains bending back on themselves; thus, the number of inter-association hydrogen bonds per unit volume in the polymer blend will be lower than that for the model compound. For an infinite chain, γ is surprisingly large, approaching 0.38 in the melt state; for real chains, however, the value is closer to 0.3 [49]. Moreover, the spacing between the functional groups along a polymer chain and the presence of bulky side groups can also significantly reduce the inter-association hydrogen bonding per unit volume, as a result of a so-called functional group accessibility effect [33]. This effect is also considered to be the origin of steric crowding and shielding [50]. Table 3 lists all the parameters required by the PCAM to estimate the thermodynamic properties for these polymer blends.

Fig. 16 displays the miscibility window for the A-PS/T-PBMA blends as predicted theoretically using the PCAM [24]. The *x*-axis represents the weight percentage of VBA in the A-PS copolymer; the *y*-axis represents the weight percentage of VBT in the T-PBMA copolymer. The plot suggests that binary blends of copolymers would be completely miscible if the VBA and VBT contents were greater than 18 wt% (ca. 8 and 11 mol%, respectively). Clearly, the model's predicted miscibility window compares favorably with our experimental results derived from DSC analyses.

4. Conclusion

We have used free radical polymerization to synthesize nucleobase (A and T)-functionalized random copolymers. Incorporating these multiple hydrogen bonding units into previously immiscible binary blends of PS and PBMA enhanced the miscibility and dramatically increased the viscosity as a result of the formation of supramolecular polymers, the presence of which we confirmed through SEC and DLS analyses. The miscibility of PS and PBMA was enhanced when the VBA and VBT units were incorporated at quite low contents of 8 and 11 mol%, respectively, into the PS and PBMA main chains, respectively, because of the high degree of inter-association resulting from the formation of an associated A–T phase. The PCAM predicted the miscibility behavior of this blend system quite well.

Acknowledgment

This work was supported financially by the National Science Council, Taiwan, Republic of China, under Contract Nos. NSC 97-2221-E-110-013-MY3 and NSC 97-2120-M-009-003.

References

[1] Park P, Zimmerman SC. J Am Chem Soc 2006;128:11582.
[2] Kim JK, Jang J, Lee DH, Ryu DY. Macromolecules 2004;37:8599.
[3] Jeon HK, Kim JK. Macromolecules 2000;30:8200.
[4] Kuo SW, Chang FC. Macromolecules 2001;34:5224.
[5] Kuo SW, Chang FC. Macromolecules 2001;34:4089.
[6] Kuo SW, Huang WJ, Huang CF, Chan SC, Chang FC. Macromolecules 2004;37:4164.
[7] Huang H, Hu Y, Zhang J, Sato H, Zhang H, Noda I, et al. J Phys Chem B 2005;109:19175.
[8] He Y, Zhu B, Inoue Y. Prog Polym Sci 2004;29:1021.
[9] Jiang M, Mei L, Xiang M, Zhou H. Adv Polym Sci 1999;146:121.
[10] Chen D, Jiang M. Acc Chem Res 2005;38:494.
[11] Yi JZ, Goh SH, Wee ATS. Macromolecules 2001;34:4662.
[12] Chien YY, Perace EM, Kwei TK. Macromolecules 1988;21:1616.
[13] Kuo SW, Chang FC. Polymer 2001;42:9843.
[14] Kuo SW, Chang FC. Macromolecules 2001;34:7737.
[15] Kuo SW. J Polym Res 2008;15:59.
[16] de Mefathi MV, Frechet JM. J Polym 1988;29:477.
[17] Prinos A, Dompros A, Panayiotou C. Polymer 1998;39:3011.
[18] Zhu KJ, Wang LQ, Yang SL. Macromol Chem Phys 1994;195:1965.
[19] Zhuang HF, Pearce EM, Kwei TK. Macromolecules 1994;27:6398.
[20] Smith JR. Prog Polym Sci 1996;21:209.
[21] Watson JD, Berry A. DNA: the secret of life. New York: Knopf; 2003.
[22] Kyogoku Y, Lord RC, Rich A. J Am Chem Soc 1967;89:496.
[23] Mather BD, Baker MB, Beyer FL, Berg MAG, Green MD, Long TE. Macromolecules 2007;40:6834.
[24] Yamauchi K, Lizotte JR, Long TE. Macromolecules 2002;35:8745.
[25] Mather BD, Lizotte JR, Long TE. Macromolecules 2004;37:9331.
[26] Coleman MM, Graf JF, Painter PC. Specific interactions and the miscibility of polymer blends. Lancaster, PA: Technomic Publishing; 1991.
[27] Coleman MM, Painter PC. Miscible polymer blend – background and guide for calculations and design. DEStech Publications Inc; 2006.
[28] Cheng CM, Egbe MI, Grasshoff JM, Guarrera DJ, Pai RP, Warner JC, et al. J Polym Sci Part A Polym Chem 1995;33:2515.
[29] Grasshoff JM, Warner JC, Taylor LD. US Patent 5,455,349; 1995.
[30] Sedlak M, Simunek P, Antonietti M. J Heterocycl Chem 2003;40:671.
[31] Lin CL, Chen WC, Liao CS, Su YC, Huang CF, Kuo SW, et al. Macromolecules 2005;38:6435.
[32] Xu Y, Painter PC, Coleman MM. Polymer 1993;34:3010.
[33] Pehlert GJ, Painter PC, Veytsman B, Coleman MM. Macromolecules 1997;30:3671.
[34] Kuo SW, Chang FC. J Polym Sci Polym Phys Ed 2002;40:1661.
[35] Fox TG. J Appl Bull Am Phys Soc 1956;1:123.
[36] Noda I. J Am Chem Soc 1989;111:8116.
[37] Lee YJ, Kuo SW, Huang WJ, Lee HY, Chang FC. J Polym Sci Polym Phys Ed 2004;42:1127.
[38] Kuo SW, Lin HC, Huang WJ, Huang CF, Chang FC. J Polym Sci Polym Phys Ed 2006;44:673.
[39] Huang CF, Kuo SW, Lin FJ, Huang WJ, Wang CF, Chang FC. Macromolecules 2006;39:300.
[40] Kuo SW, Huang CF, Tung PH, Huang WJ, Huang JM, Chang FC. Polymer 2005;46:9348.
[41] Noda I, Ozaki Y. Two-dimensional correlation spectroscopy. John Wiley & Sons; 2004.
[42] Mathias JP, Seto CT, Simanek EE, Whitesides GM. J Am Chem Soc 1994;116:1725.
[43] Simanek EE, Isaacs L, Li X, Wang CC, Whitesides GM. J Org Chem 1997;62:8994.
[44] Tung PH, Kuo SW, Chang FC. Polymer 2007;48:3192.
[45] Painter PC, Coleman MM. Prog Polym Sci 1995;20:1.
[46] Benesi HA, Hildebrand JH. J Am Chem Soc 1949;71:2703.
[47] Park Y, Veytsman B, Coleman M, Painter PC. Macromolecules 2005;38:3703.
[48] Kuo SW, Chan SC, Wu HD, Chang FC. Macromolecules 2005;38:4729.
[49] Painter PC, Veytsman B, Kumar S, Shenoy S, Graf JF, Xu Y, et al. Macromolecules 1997;30:932.
[50] Pehlert GJ, Painter PC, Coleman MM. Macromolecules 1998;31:8423.